Hindawi
International Journal of Antennas and Propagation
Volume 2017, Article ID 3987263, 7 pages
https://doi.org/10.1155/2017/3987263

Research Article

CPW-Fed Wideband Circular Polarized Antenna for UHF RFID Applications

Sun-Woong Kim,[1] Guen-Sik Kim,[1] and Dong-You Choi[2]

[1] *Department of Information and Communication Engineering, Graduate School, Chosun University, Gwangju, Republic of Korea*
[2] *Department of Information and Communication Engineering, Chosun University, Gwangju, Republic of Korea*

Correspondence should be addressed to Dong-You Choi; dychoi@chosun.ac.kr

Received 21 March 2017; Revised 10 May 2017; Accepted 6 June 2017; Published 16 July 2017

Academic Editor: Ikmo Park

We propose a wide bandwidth antenna with a circular polarization for universal Ultra High Frequency (UHF) radio-frequency identification (RFID) reader applications. To achieve a wide 3 dB axial ratio (AR) bandwidth, three T-shaped microstrip lines are inserted into the ground plane. The measured impedance bandwidth of the proposed antenna is 480 MHz and extends from 660 to 1080 MHz, and the 3 dB AR bandwidth is 350 MHz and extends from 800 to 1155 MHz. The radiation pattern is a bidirectional pattern with a maximum antenna gain of 3.67 dBi. The overall size of the proposed antenna is $114 \times 114 \times 0.8\,\mathrm{mm}^3$.

1. Introduction

Radio-frequency identification (RFID) technology is used in devices that transmit and receive information using radio frequency (RF) from electronic tags attached to objects in various applications. The RFID frequency bands are the HF band at 13.56 MHz, UHF band from 860 to 960 MHz, and ISM band at 2.4 GHz [1, 2]. RFID applications in the UHF band use different frequency bands in different countries. The frequency bands used are as follows: 902–928 MHz in North America, 840.5–844.5 MHz and 920.5–924.5 MHz in China, 950–956 MHz in Japan, 866–869 MHz in Europe, 920–926 MHz in Australia, 865–867 MHz band in India, and 908.5–914 MHz in South Korea [3–5]. The (UHF) RFID full coverage band in each country is about 840–960 MHz.

In the UHF band RFID system, the antenna plays an important role in the communications between the reader and tag. The characteristics of the antenna determine the recognition distance between the reader and the tag. To maximize the distance, the return loss characteristics of the antenna should be as small as possible in the operating frequency band, and the antenna should be designed with a circular polarization [6–8].

In this paper, we describe the design and fabrication of an antenna with circular polarization for an RFID reader in the UHF band. In terms of impedance matching, we used three microstrip lines to achieve an impedance of −10 dB across the wide application band. We also used a T-shaped microstrip line to induce a circular polarization characteristic.

2. Antenna Design

The structure of the proposed antenna is shown in Figure 1. It was fabricated using an FR4 substrate with a relative permittivity of 4.5, loss tangent of 0.02, and thickness of 0.8 mm. The substrate was square with a side length G, and the overall size was $114 \times 114\,\mathrm{mm}^2$ [9–11]. The feed structure of the antenna used a coplanar waveguide (CPW) structure. The geometric parameters of the L-shaped microstrip lines were L_2, L_{2_1}, W_2, and W_{2_1}. For impedance matching, we used three microstrip lines with geometric parameters of L_3, L_{3_1}, L_{3_2}, and W_3. The geometric parameters of the T-shaped microstrip line used for the circular polarization were L_1, L_{1_1}, and W_1. The fabricated antenna is shown in Figure 2.

The design process used for the antenna consisted of three steps, which are illustrated in Figure 3.

The reflection coefficients and axial ratio (AR) simulation characteristics of the three steps were analyzed using HFSS version 12, and the results are shown in Figure 4.

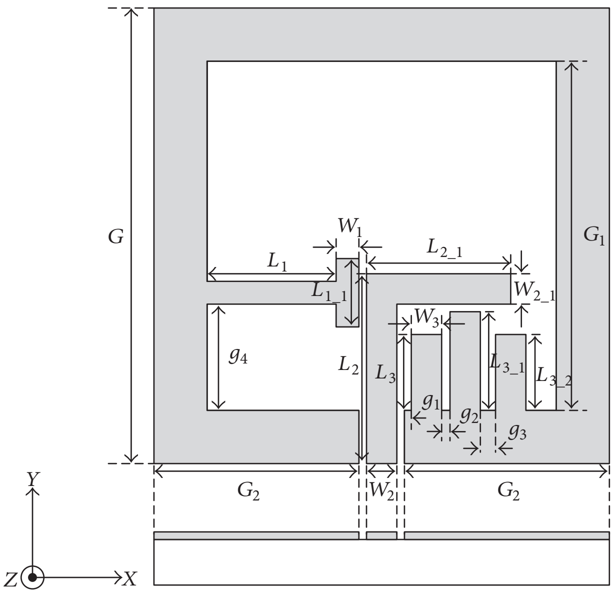

Figure 1: Structure and dimensions (in mm) of the proposed antenna: $G = 114$, $G_1 = 86$, $G_2 = 53$, $L_1 = 35$, $L_{1\_1} = 16$, $W_1 = 4$, $L_2 = 45$, $W_2 = 5$, $L_{2\_1} = 35$, $W_{2\_1} = 5$, $L_3 = 20$, $L_{3\_1} = 24$, $L_{3\_2} = 15$, $W_3 = 5$, $g_1 = 0.5$, $g_2 = 2$, $g_3 = 3$, and $g_4 = 25$.

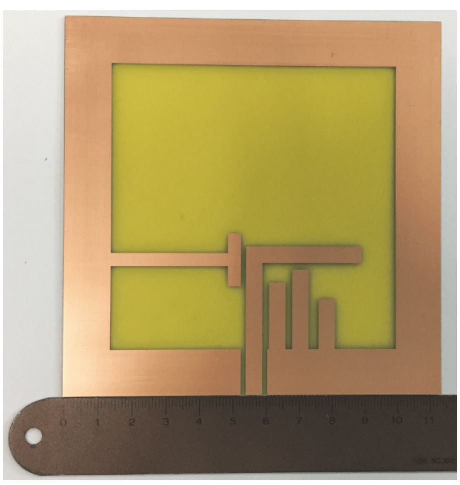

Figure 2: Photograph of the fabricated antenna.

Antenna 1 is a basic antenna with a CPW L-shaped feed structure. It exhibited a good impedance matching characteristic, and a −10 dB reflection coefficient bandwidth was achieved over a wide bandwidth of 331 MHz from 739 to 1070 MHz. However, it did not achieve the desired 3 dB axial ratio bandwidth (ARBW). In Antenna 2, a T-shaped microstrip line was added to improve the 3 dB AR characteristics. The resulting antenna exhibited a suitably wide bandwidth of 345 MHz from 772 to 1117 MHz, although the impedance matching was poor. Therefore, in Antenna 3, the impedance was connected to the ground of the three microstrip lines. As a result, a −10 dB reflection coefficient bandwidth of 480 MHz from 714 to 1194 MHz was achieved, and the 3 dB ARBW was 380 MHz from 775 to 1155 MHz.

Table 1: Detailed results of the proposed antenna for various T-shaped microstrip line lengths.

L_1 (mm)	L_2 (mm)	3 dB ARBW (MHz)
35	10	209
35	12	212
35	14	291
35	**16**	**380**
35	18	338
35	20	342

The 3 dB ARBW results for the values of L_1, L_2 of the T-shaped microstrip line are shown in Figures 5(a) and 5(b). The analyzed 3 dB ARBW values along with the tested values of L_1 and L_2 are listed in Table 1. As shown in the table, better results were observed when the values of L_1 and L_2 were 35 and 16, respectively. The corresponding measured 3 dB ARBW value was 380 MHz, which is considered to be a good result based on our earlier discussion.

3. Experiment Results and Analysis

The impedance bandwidth of the manufactured antenna was measured using a Network Analyzer (Agilent Co.), and the results are shown in Figure 6.

The simulated −10 dB reflection coefficient bandwidth of the proposed antenna extended from 714 to 1194 MHz (480 MHz), and the fractional bandwidth was 50.3%. The measured −10 dB reflection coefficient bandwidth of the manufactured antenna was 660–1080 MHz (420 MHz), and the fractional bandwidth was 48.27%.

The simulated and measured 3 dB ARBW results of the manufactured antenna are shown in Figure 7.

The simulated 3 dB ARBW of the proposed antenna is 775–1155 MHz (380 MHz), and the measured 3 dB ARBW of the manufactured antenna is about 800–1150 MHz (350 MHz).

The radiation pattern of both simulated and measured values, for the XZ- and YZ-planes in the 800–1100 MHz band, and the results are shown in Figure 8.

The radiation pattern of the proposed antenna exhibited good bidirectional characteristics.

In addition, right-hand circular polarized radiation (RHCP) was radiated along the front side of the proposed antenna, and left-hand circular polarized radiation was radiated along the back side of the proposed antenna. The maximum gain of the proposed antenna (RHCP and LHCP) was concentrated along the $+z$-axis and $-z$-axis.

The gain and radiation efficiency results of the proposed antenna are shown in Figure 9.

The gain analysis results fluctuated between 3.4 and 3.8 dBi from 750 to 1000 MHz. The measured maximum gain was 3.67 dBi at 750 MHz, and the simulated maximum gain of 3.8 dBi was observed at 1000 MHz. The proposed antenna observed a radiation efficiency of over 90% in impedance bandwidth both simulated and measured results.

The comprehensive results of the proposed antenna are listed in Table 2 and include a wide bandwidth and measured

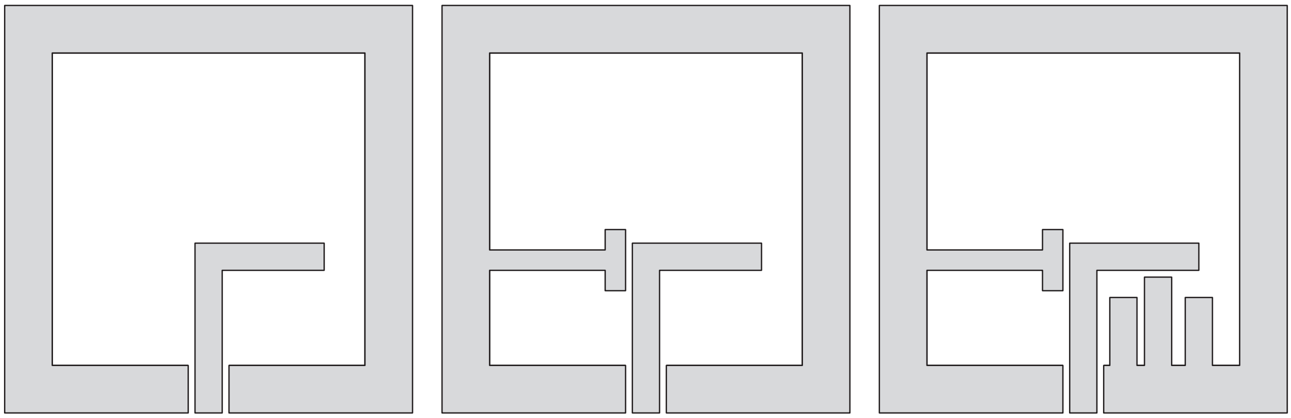

(a) Antenna 1 (b) Antenna 2 (c) Antenna 3 (proposed)

Figure 3: Three steps in the antenna design process.

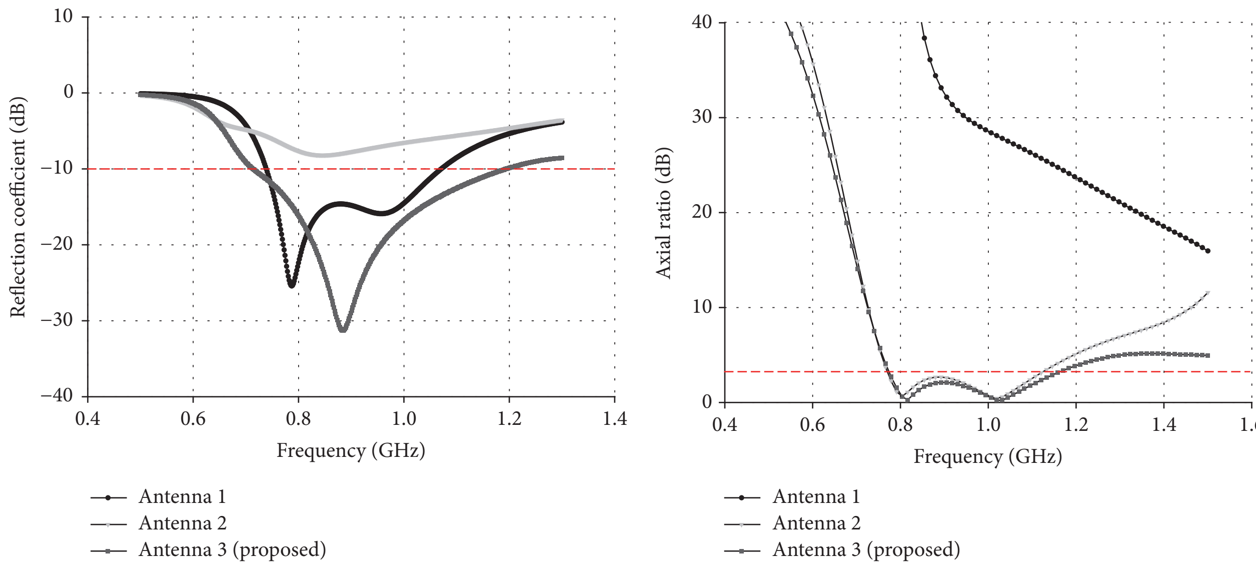

(a) Reflection coefficient (b) Axial ratio

Figure 4: Simulation analysis results of the three methods.

Table 2: Comprehensive results of the proposed antenna.

	Simulated	Measured
−10 dB reflection coefficient range [MHz]	714–1194	660–1080
Impedance bandwidth [MHz]	480	420
Fractional bandwidth [%]	50.3	48.27
Resonant frequency [MHz]	1000	900
Maximum gain [dBi]	3.8	3.67

and simulated gain results that were in good agreement. However, there were subtle differences between the simulated and measured results. There were two reasons for these differences. The first was an error during the manufacturing process, and the second was loss between the antenna and connector. The subtle difference is not a problem at the performance of the proposed antenna.

The proposed antenna is compared to other antennas with UHF band for RFID reader in Table 3. The advantage of the proposed antenna lies in its wideband bandwidth and the fact that it has a relatively small size. In order to achieve the proposed antenna, a wide ARBW and wide impedance bandwidth through three microstrip lines and T-shaped microstrip lines are used.

4. Conclusion

The proposed antenna exhibited circular polarized wideband characteristics. A T-shaped microstrip line induced the circular polarization characteristics and 3 dB ARBW. In addition, the wideband characteristics were matched due to the three microstrip lines. The overall size of the fabricated antenna was $114 \times 114 \times 0.8\,\text{mm}^3$.

The measured impedance bandwidth (−10 dB reflection coefficient) results were 420 MHz from 660 to 1080 MHz, and

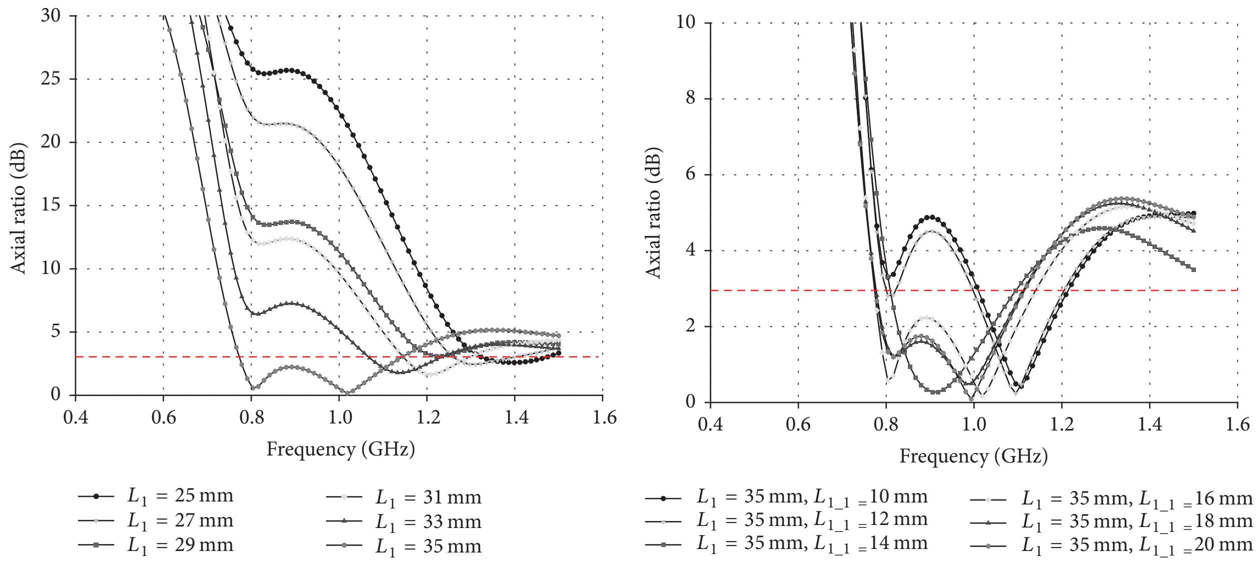

(a) L_1 (b) L_2

Figure 5: Three dB axial ratios of the proposed antenna with various L_1, L_{1_1} values.

Table 3: Comparison of the proposed antenna and different antenna.

Antennas	−10 dB S_{11} BW [MHz]	3 dB ARBW [MHz]	Gain [dBi]	Dimensions [mm^3]
[3]	904–941/37	918–929/11	3.8	90 × 90 × 4.572
[4]	618–998/480	791–1123/332	3.4	120 × 120 × 0.8
[12]	860–930/70	—	3.7	110 × 110 × 5
[13]	891–928/37	907–915/8	5.85	54 × 54 × 1.6
[14]	820–880/60 830–928/98	864–887/19 899–913/14	1.6	90 × 90 × 1.6
[15]	902–928/26	900–936/36	1.35	105 × 90 × 1.6
Proposed antenna	660–1080/420	775–1155/380	3.67	114 × 114 × 0.8

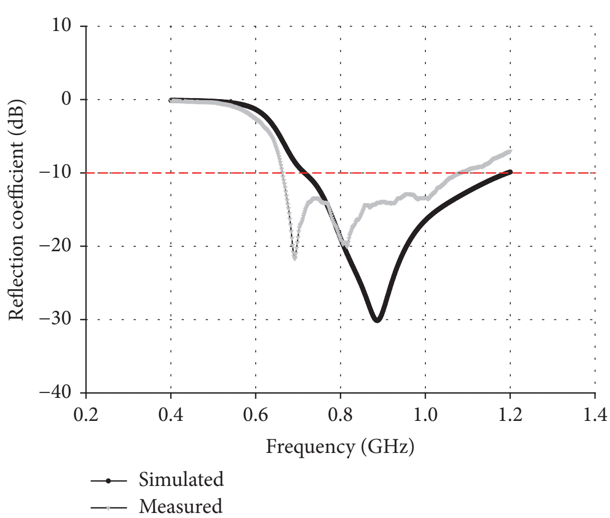

Figure 6: Simulated and measured reflection coefficient results of the manufactured antenna.

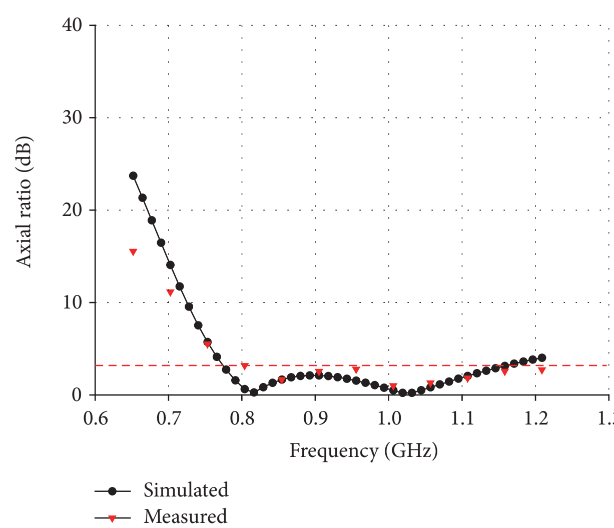

Figure 7: Simulated and measured AR bandwidth results of the manufactured antenna.

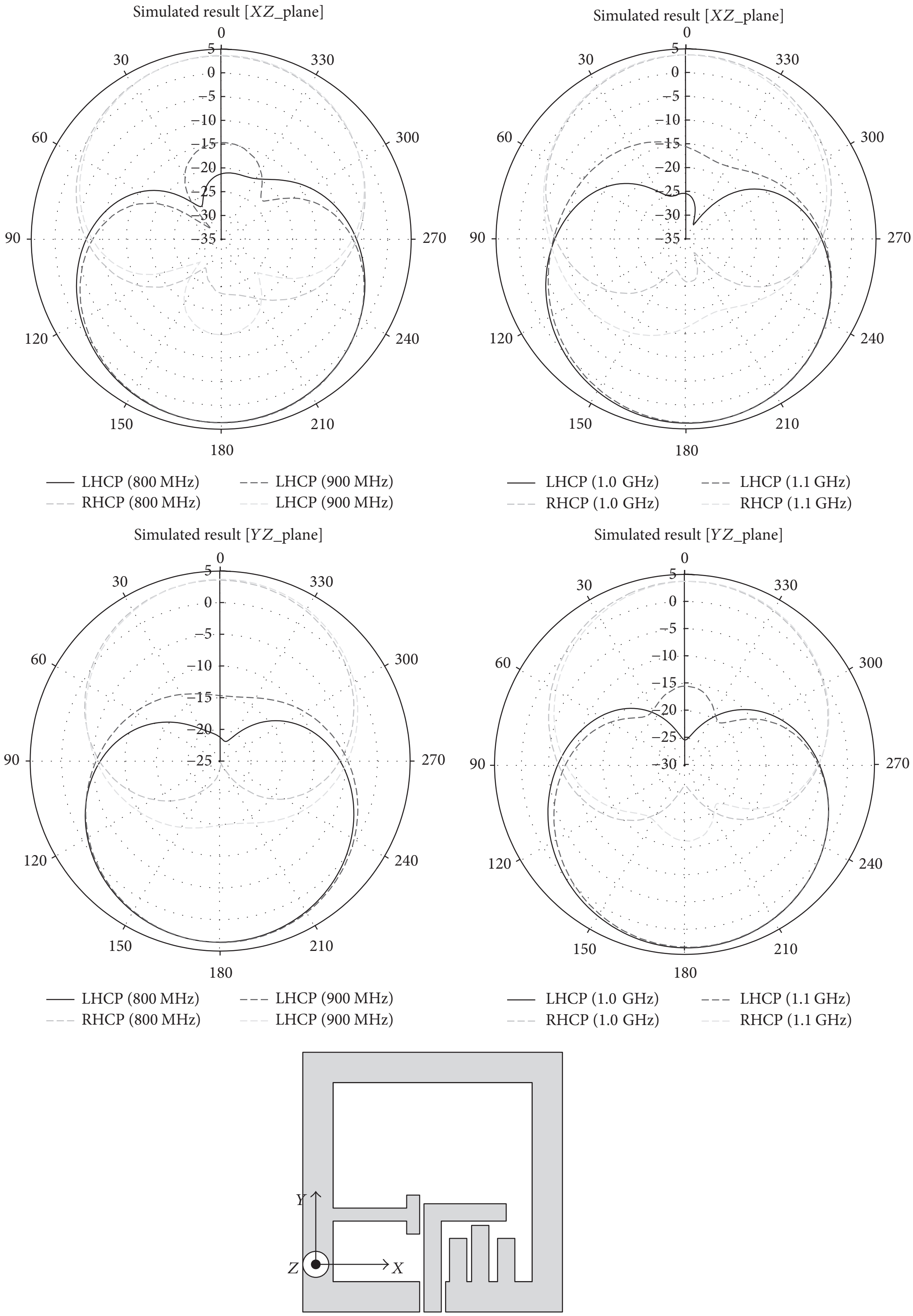

(a) Simulated radiation pattern result

Figure 8: Continued.

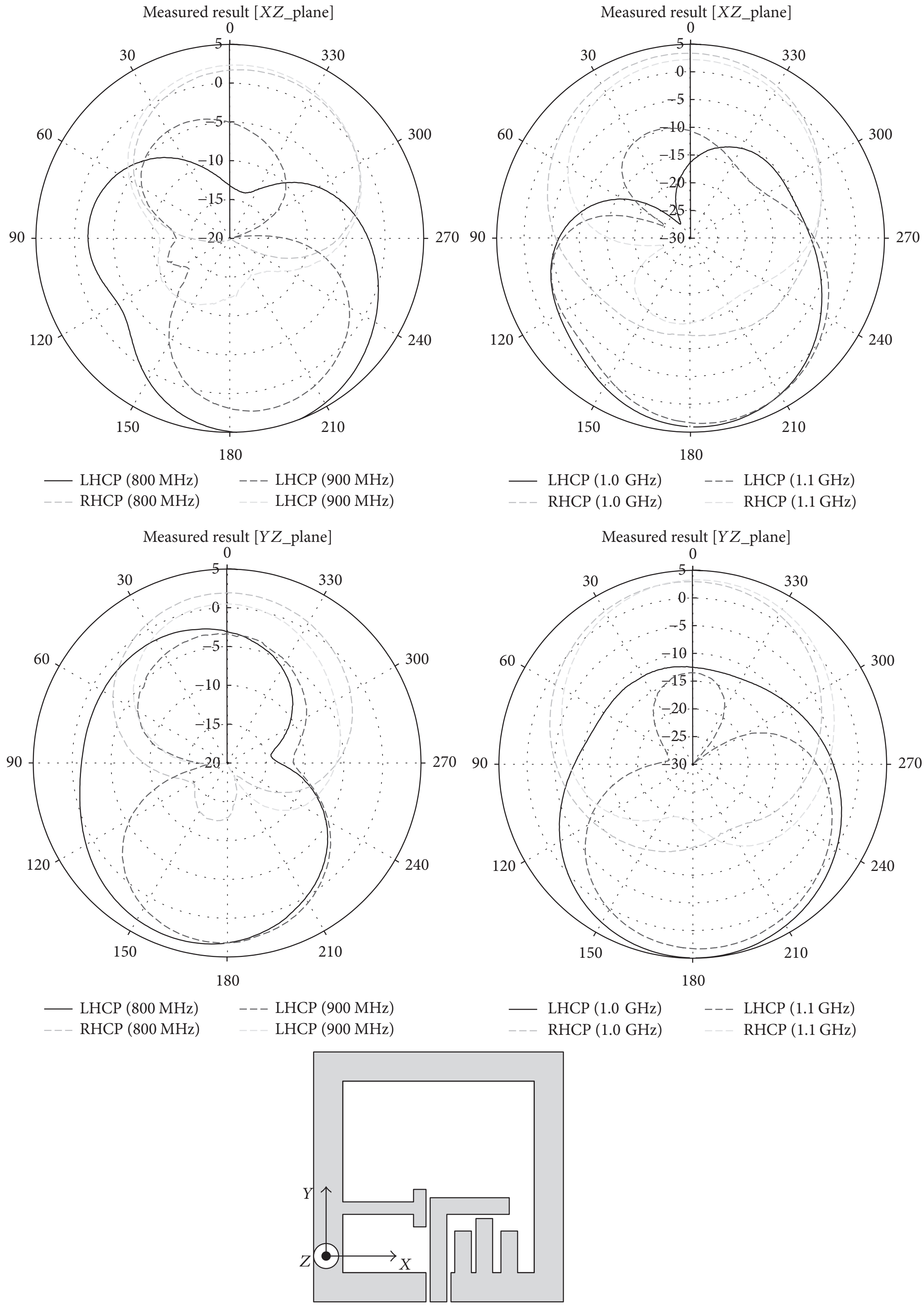

(b) Measured radiation pattern result

FIGURE 8: Radiation pattern of the manufactured antenna.

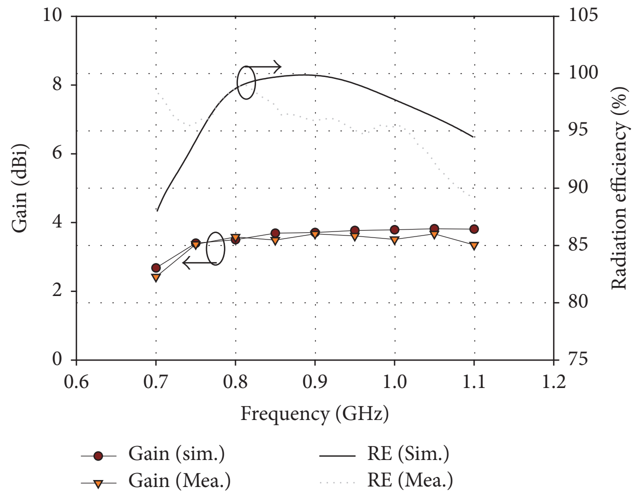

Figure 9: Gain and radiation efficiency results of the manufactured antenna.

the 3 dB ARBW results were 350 MHz from 800 to 1155 MHz. The analysis of the radiation pattern showed a bidirectional pattern and a maximum measured antenna gain of 3.67 dBi.

The results of a comprehensive analysis of both the measurements and simulation were in good agreement.

Conflicts of Interest

The authors declare that they have no conflicts of interest.

Acknowledgments

This research was supported by the Basic Science Research Program through the National Research Foundation of Korea (NRF) funded by the Ministry of Education (2016R1D1A1B03931806).

References

[1] J. Lim, B. Kang, J. Jwa, H. Kim, and D. Yang, "RFID Reader antenna with hilbert curve fractal structure over partially grounded plane," *The Journal of the Korea Contents Association*, vol. 7, no. 4, pp. 30–38, 2007.

[2] Y. Jin, J. Tak, and J. Choi, "Quadruple band-notched trapezoid UWB antenna with reduced gains in notch bands," *Journal of Electromagnetic Engineering and Science*, vol. 16, no. 1, pp. 35–43, 2016.

[3] Nasimuddin, Z. N. Chen, and X. Qing, "Asymmetric-circular shaped slotted microstrip antennas for circular polarization and RFID applications," *IEEE Transactions on Antennas and Propagation*, vol. 58, no. 12, pp. 3821–3828, 2010.

[4] R. Cao and S.-C. Yu, "Wideband compact CPW-fed circularly polarized antenna for universal UHF RFID reader," *IEEE Transactions on Antennas and Propagation*, vol. 63, no. 9, pp. 4148–4151, 2015.

[5] J. H. Yoon, S. J. Ha, and Y. C. Rhee, "A novel monopole antenna with two arc-shaped strips for WLAN/WiMAX application," *Journal of Electromagnetic Engineering and Science*, vol. 15, no. 1, pp. 6–13, 2015.

[6] J. H. Ju and J. H. Chun, "A study on the antenna design of the RFID reader for 900 MHz band," *Journal of Communications and Networks*, vol. 33, no. 12, pp. 473–478, 2008.

[7] S.-W. Kim and D.-Y. Choi, "Compact filtering monopole patch antenna with dual-band rejection," *SpringerPlus*, vol. 5, no. 1, article no. 883, 2016.

[8] S.-W. Kim and D.-Y. Choi, "Implementation of rectangular slit-inserted ultra-wideband tapered slot antenna," *SpringerPlus*, vol. 5, no. 1, article no. 1387, 2016.

[9] S. Kim, K. Kwon, and J. Choi, "A compact circularly-polarized antenna with enhanced bandwidth for WBAN applications," *Microwave and Optical Technology Letters*, vol. 55, no. 8, pp. 1738–1741, 2013.

[10] G. Pan, Y. Li, Z. Zhang, and Z. Feng, "A compact wideband slot-loop hybrid antenna with a monopole feed," *IEEE Transactions on Antennas and Propagation*, vol. 62, no. 7, pp. 3864–3868, 2014.

[11] K. J. Kim, W. C. Choi, and Y. J. Yoon, "Circularly rotated array for dual polarized applicator in superficial hyperthermia system," *Journal of Electromagnetic Engineering and Science*, vol. 15, no. 1, pp. 20–25, 2015.

[12] Z.-J. Tang, J. Zhan, and H.-L. Liu, "Dual-resonance compact circularly polarized reader antenna for UHF RFID applications," *Microwave and Optical Technology Letters*, vol. 54, no. 11, pp. 2531–2533, 2012.

[13] A. Farswan, A. K. Gautam, B. . Kanaujia, and K. Rambabu, "Design of Koch fractal circularly polarized antenna for handheld UHF RFID reader applications," *IEEE Transactions on Antennas and Propagation*, vol. 64, no. 2, pp. 771–775, 2016.

[14] R. Cao and C. Kai Wang, "Frequency-reconfigurable circularly polarized antenna for UHF RFID reader," *Microwave and Optical Technology Letters*, vol. 58, no. 12, pp. 2842–2845, 2016.

[15] C. Raviteja, C. Varadhan, M. Kanagasabai, A. K. Sarma, and S. Velan, "A fractal-based circularly polarized UHF RFID reader antenna," *IEEE Antennas and Wireless Propagation Letters*, vol. 13, pp. 499–502, 2014.